

SCIENTIFIC REPORTS



OPEN

SDS-PAGE analysis of A β oligomers is disserving research into Alzheimer's disease: appealing for ESI-IM-MS

Received: 21 May 2015
Accepted: 09 September 2015
Published: 09 October 2015

Rosa Pujol-Pina^{1,*}, Sílvia Vilaprinyó-Pascual^{1,*}, Roberta Mazzucato¹, Annalisa Arcella², Marta Vilaseca³, Modesto Orozco^{2,4} & Natàlia Carulla¹

The characterization of amyloid-beta peptide (A β) oligomer forms and structures is crucial to the advancement in the field of Alzheimer's disease (AD). Here we report a critical evaluation of two methods used for this purpose, namely sodium dodecyl sulfate polyacrylamide gel electrophoresis (SDS-PAGE), extensively used in the field, and ion mobility coupled to electrospray ionization mass spectrometry (ESI-IM-MS), an emerging technique with great potential for oligomer characterization. To evaluate their performance, we first obtained pure cross-linked A β ₄₀ and A β ₄₂ oligomers of well-defined order. Analysis of these samples by SDS-PAGE revealed that SDS affects the oligomerization state of A β ₄₂ oligomers, thus providing flawed information on their order and distribution. In contrast, ESI-IM-MS provided accurate information, while also reported on the chemical nature and on the structure of the oligomers. Our findings have important implications as they challenge scientific paradigms in the AD field built upon SDS-PAGE characterization of A β oligomer samples.

A β oligomers, species that form early during A β aggregation, are considered the pathogenic molecular form of A β in AD¹. Consequently, they have been singled out as a target to treat this disease². However, the characterization of A β oligomers is challenging because they are heterogeneous—comprising a range of aggregation states—and because they form transiently—evolving as a function of time^{3,4}. In spite of these difficulties, different approaches and techniques have been developed to characterize them^{5–12}. One such approach relies on the production of cross-linked oligomers by means of the photo-induced cross-linking of unmodified proteins (PICUP) reaction, and their subsequent analysis by SDS-PAGE (Fig. 1)^{5,13}. A β ₁₋₄₀ (A β ₄₀) and A β ₁₋₄₂ (A β ₄₂) are the two principal forms of A β , differing by only two hydrophobic residues at the C-terminus. Analysis of PICUP cross-linked A β ₄₀ and A β ₄₂ samples by SDS-PAGE revealed that A β ₄₀ oligomerizes through dimers up to tetramers while A β ₄₂ does so mainly through pentamers and hexamers^{5,13}. Since A β ₄₂ has been shown to have a more prominent role in AD^{14,15}, PICUP/SDS-PAGE analysis led to the conclusion that pentamers and hexamers constituted the basic building blocks for A β aggregation^{5,13}.

The importance of pentamers and hexamers in A β aggregation has become a scientific paradigm in the field. For example, according to the Web of Science, there are six key papers^{7–9,16–18}, frequently cited together (more than one thousand times), that constitute the foundational core for the research front entitled “A β oligomers, fibrils and AD”. Three of these six papers are based directly^{16,18} or indirectly⁷ on

¹Institute for Research in Biomedicine (IRB Barcelona), Baldiri Reixac 10, Barcelona 08028, Spain. ²Joint IRB-BSC Research Program in Computational Biology, Institute for Research in Biomedicine (IRB Barcelona), Baldiri Reixac 10, Barcelona 08028, Spain. ³Mass Spectrometry Core Facility, Institute for Research in Biomedicine (IRB Barcelona), Baldiri Reixac 10, Barcelona 08028, Spain. ⁴Department of Biochemistry and Molecular Biology, University of Barcelona, Diagonal 647, Barcelona 08028, Spain. *These authors contributed equally to this work. Correspondence and requests for materials should be addressed to N.C. (email: natalia.carulla@irbbarcelona.org)

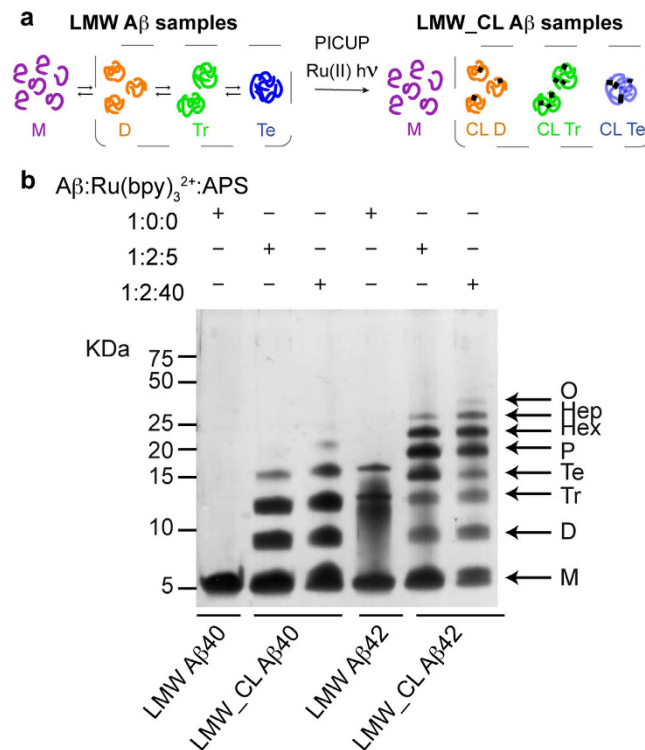


Figure 1. PICUP and SDS-PAGE analysis apparently indicate that A β 40 and A β 42 oligomerize through distinct pathways. (a) LMW A β samples contain monomers in equilibrium with low order A β oligomers (left). Synthetic LMW_CL A β samples are obtained by subjecting their LMW counterparts to PICUP (right). (b) Characterization of LMW and LMW_CL A β 40 and A β 42 oligomer distribution by SDS-PAGE analysis. LMW_CL A β 40 and A β 42 samples were prepared using two different A β /Ru(bpy)₃²⁺/APS ratios, namely 1:2:5 and 1:2:40.

the conclusions derived from PICUP/SDS-PAGE analysis. However, SDS-PAGE analysis might be biased since SDS has been suggested to affect the oligomerization state of A β , especially that of A β 42^{8,19,20}. Given the potential artifacts of SDS, it is critical to evaluate the usefulness of SDS-PAGE to characterize A β oligomers to have a criteria with which to revise the conclusions derived from its use. For the purpose of this evaluation, it is important to consider new techniques that are not dependent on SDS. ESI-IM-MS is an emerging method with great potential for the characterization of oligomers^{7,10,21–24}. ESI-IM-MS offers the possibility to resolve heterogeneous oligomer samples on the basis of differences in the order and/or in the structure of the oligomers present in a sample. Moreover, the time scale of IM experiments (tens of ms) is much shorter than that of conventional structural techniques (s to hrs), thus making them ideal for the structural characterization of heterogeneous and dynamic samples such as A β oligomers. Furthermore, since ESI-MS allows the preservation of many non-covalent interactions within complexes²⁵, even several involving a reduced interaction surface^{26–30}, ESI-IM-MS emerges as a suitable method for the characterization of not only cross-linked oligomers but also non-covalent ones.

Here we provide a critical evaluation of SDS-PAGE and ESI-IM-MS for the characterization of A β oligomers. To this end, we first developed a protocol to obtain pure PICUP cross-linked (CL) A β 40 and A β 42 oligomers of defined order. Using these samples, we unequivocally established that SDS-PAGE leads to artifacts in determining the order and distribution of A β 42 oligomers. On the other hand, ESI-IM-MS was further established as a reliable technique through which to characterize the order, distribution, chemical modifications, and structure of both covalently and non-covalently linked A β oligomers. Our results have important implications as they challenge previous scientific paradigms in the field built upon results obtained through the SDS-PAGE characterization of A β oligomers. In this context, we demonstrate that pentamers and hexamers are artifacts of SDS-PAGE analysis. Moreover, we identify A β 40 and A β 42 dimers and trimers, adopting a globular structure and lacking defined secondary structure, as the earliest forms to be considered in the design of therapeutic strategies targeting A β oligomerization.

Results

PICUP and SDS-PAGE apparently indicate that A β 40 and A β 42 oligomerize through distinct pathways. Following previously described protocols^{31,32}, we obtained A β 40 and A β 42 samples in their lowest aggregation state using size exclusion chromatography (SEC). We refer to these samples as low molecular weight (LMW) A β 40 and A β 42 (Fig. 1a), as various techniques have shown that they

comprise monomers in rapid equilibrium with low order oligomers³¹. To freeze this dynamic equilibrium, LMW A β samples were cross-linked by means of PICUP^{5,13}. We refer to these samples as LMW cross-linked (LMW_CL) A β 40 and A β 42 (Fig. 1a). Initially, we used previously described conditions—an A β /tris(bipyridyl) Ru(II) complex (Ru(bpy)₃²⁺)/ammonium persulfate (APS) ratio of 1:2:40—to obtain LMW_CL A β 40 and A β 42^{5,13,33}. Analysis of these samples by SDS-PAGE and silver staining reproduced previous results described in the literature (Fig. 1b). Uncross-linked LMW A β 40 ran with a molecular weight consistent with that of monomers. LMW_CL A β 40 presented an oligomer distribution characterized by monomers through to pentamers—displaying decreasing intensity with increasing oligomer order. Uncross-linked A β 42 produced predominantly three bands consistent with monomers, trimers and tetramers. LMW_CL A β 42 ran as monomers through to trimers—displaying decreasing intensity with increasing oligomer order—and as a Gaussian-like distribution comprising tetramers through to octamers, with a maximum at pentamers and hexamers. These results apparently support the hypothesis from Teplow and co-workers that A β 40 and A β 42 oligomerize through distinct pathways^{5,13}.

To determine the homogeneity of the LMW_CL A β samples, we analyzed LMW_CL A β 40 by reversed phase high-pressure liquid chromatography (RP-HPLC) and LC coupled to high resolution MS (LC-HRMS). This analysis revealed that an A β /Ru(bpy)₃²⁺/APS ratio of 1:2:40 led to various degrees of oxidized byproducts (Supplementary Fig. S1a and Table S1). We then optimized PICUP conditions and found that an A β /Ru(bpy)₃²⁺/APS ratio of 1:2:5 largely overcame the formation of these byproducts (Supplementary Fig. S1b,c). Although the optimized conditions led to a lower yield of cross-linked oligomers (Fig. 1b), they were used throughout our study since they ensured chemically well-defined CL A β oligomers.

A β 42 pentamers and hexamers are artifacts of SDS-PAGE analysis. Various studies have suggested that SDS affects the oligomerization state of A β samples^{8,19,20}. To address this possibility, we sought to determine the oligomer order and distribution of LMW_CL A β samples using a new strategy that involved the same principles as those used in SDS-PAGE, that is, denaturation/disaggregation followed by size fractionation, but without using SDS. Denaturation/disaggregation was accomplished by lyophilizing LMW and LMW_CL A β 40 and A β 42 samples and later resuspending them in 6.8 M guanidine thiocyanate (GdnHSCN), conditions used to solubilize plaque cores³⁴. Therefore, treatment of LMW and LMW_CL A β samples with 6.8 M GdnHSCN should break all non-covalent A β -A β interactions preserving only the covalent ones formed during the cross-linking reaction. Size fractionation of the resulting oligomers was attained by SEC using 10 mM ammonium acetate at pH 8.5 as the elution buffer. This buffer was chosen because it prevented aggregation of the samples during SEC fractionation. After this treatment, referred to as GdnHSCN-SEC analysis, LMW A β 40 and A β 42 eluted as a single peak (Fig. 2a,b), confirming that GdnHSCN broke all the non-covalent interactions and that aggregation was prevented during SEC fractionation. In contrast, LMW_CL A β 40 and A β 42 samples eluted as four main peaks (Fig. 2c,d). ESI-MS analysis confirmed that the peaks eluting at 39.5, 34.7, and 32.6 mL in LMW_CL A β 40 and at 38.4, 33.5, and 31.6 mL in LMW_CL A β 42 samples corresponded to “monomers”, CL dimers, and CL trimers of A β 40 (Fig. 2e) and A β 42 (Fig. 2f), respectively. Although peaks eluting at 31.3 mL in LMW_CL A β 40 (Fig. 2c) and at 30.5 mL in LMW_CL A β 42 (Fig. 2d) samples were low in abundance, ESI-MS analysis revealed the presence of +8 and +7 charge states corresponding to tetramers. Of note, ESI-MS analysis of peaks corresponding to “monomers” in LMW and LMW_CL A β samples also showed that they contained charge states corresponding to non-covalent dimers and trimers (Fig. 2e,f). These observations are consistent with previous results indicating that A β monomers exist in rapid equilibrium with low order A β oligomers (Fig. 1a)³¹. Altogether, GdnHSCN-SEC analyses indicated that the oligomer distribution for LMW_CL A β 40 and A β 42 samples was the same, comprising dimers, trimers and tetramers (Fig. 2c,d). This result is inconsistent with that obtained when the same samples were analyzed by SDS-PAGE (Fig. 1b), thus suggesting that SDS affects A β oligomerization, particularly that of A β 42.

Having access to pure synthetic CL A β oligomer samples of well-defined order offered us a unique opportunity to study the effect of SDS on A β oligomerization. We analyzed isolated CL A β 40 and A β 42 dimers and trimers as well as mixtures of them, obtained after GdnHSCN-SEC, by SDS-PAGE. CL A β 40 dimers and trimers ran as expected (Fig. 2g). However, CL A β 42 dimers run also as tetramers, CL A β 42 trimers also as hexamers, and mixtures of CL A β 42 dimers and trimers also as tetramers, pentamers and hexamers (Fig. 2h). These findings have two important implications: i) SDS is responsible for affecting the oligomerization state of A β 42 oligomers. In fact, the temperature and incubation time prior to SDS-PAGE analysis did not have an effect in the oligomerization state of the samples (Supplementary Fig. S2). Consequently, SDS-PAGE is not a reliable technique to characterize the order and distribution of A β oligomers present in a sample; ii) they challenge the widely accepted view that pentamers and hexamers are the basic building blocks for A β aggregation.

ESI-IM-MS analysis reveals that A β 40 and A β 42 predominantly oligomerize through dimers and trimers. Given that SDS-PAGE analysis leads to artifacts in the characterization of A β oligomers, we consider it critical to establish techniques that can provide reliable results. As detailed in the introduction, ESI-IM-MS is an emerging technique with great potential to characterize the oligomers present in a sample^{7,10,22}, circumventing the problems associated with the use of SDS^{8,19,20}. To evaluate the feasibility

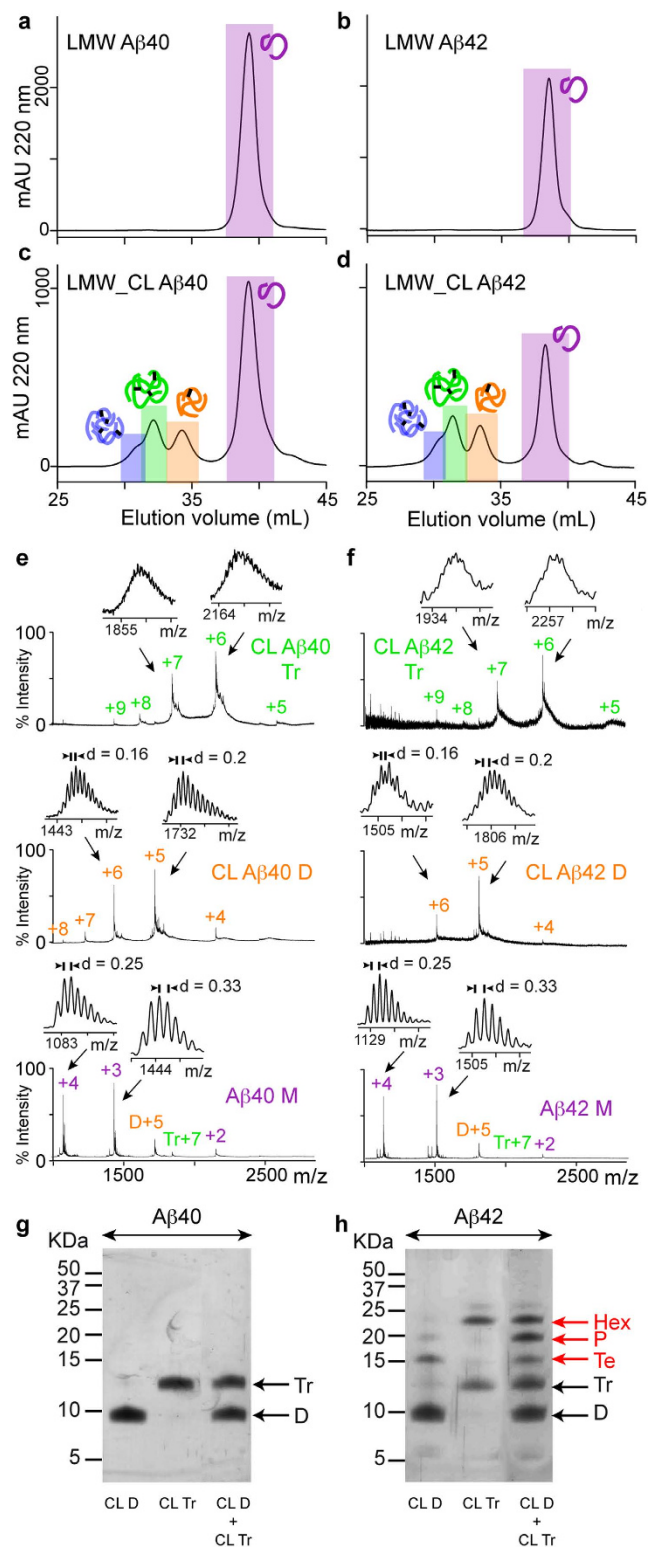


Figure 2. A β 42 pentamers and hexamers are artifacts of SDS-PAGE analysis. GdnHSCN-SEC analysis of (a) LMW A β 40, (b) LMW A β 42, (c) LMW_CL A β 40, and (d) LMW_CL A β 42. ESI-MS spectra corresponding to peaks detected after GdnHSCN-SEC analysis of (e) LMW_CL A β 40 and (f) LMW_CL A β 42 samples. SDS-PAGE analysis of isolated CL dimers and trimers, as well as mixtures of them for (g) A β 40 and (h) A β 42 obtained after GdnHSCN-SEC fractionation. M = monomers, D = dimers, Tr = trimers, Te = tetramers, P = pentamers, and Hx = hexamers. The red arrows indicate oligomers formed artifactually in the presence of SDS.

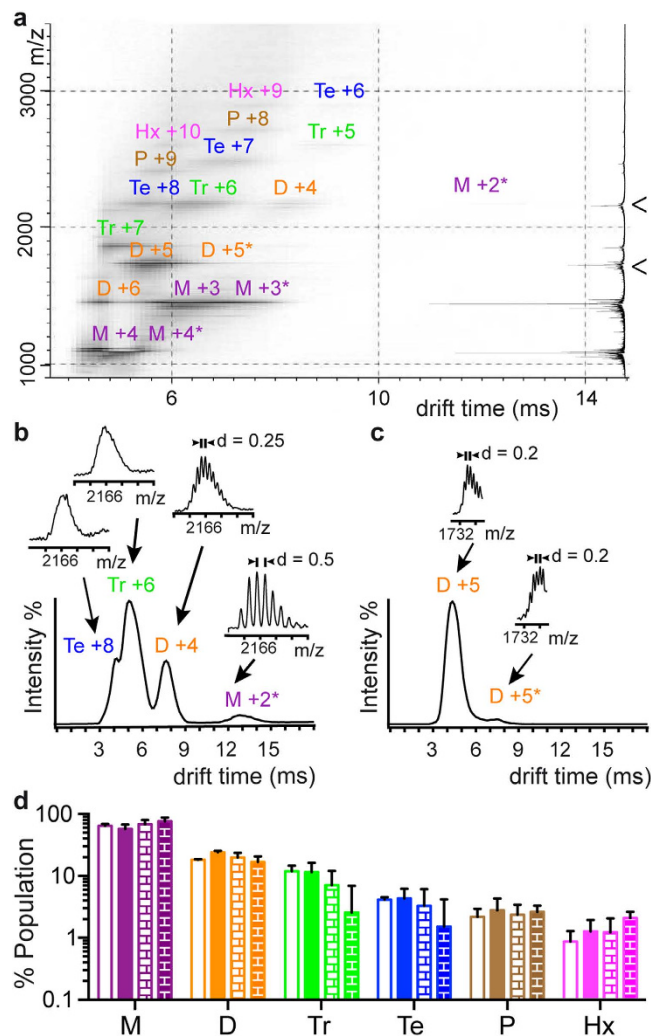


Figure 3. ESI-IM-MS analysis reveals that A β 40 and A β 42 oligomerize predominantly through dimers and trimers. (a) ESI-IM-MS spectra for LMW A β 40. M = monomers, D = dimers, Tr = trimers, Te = tetramers, P = pentamers, and Hx = hexamers. The number adjacent to each aggregation state refers to the charge state of the ion. The summed m/z spectrum is shown on the right. Projections of the ESI-IM-MS spectra on the drift time axis for (b) m/z 2166 (M + 2, D + 4, Tr + 6, and Te + 8) and (c) m/z 1732 (D + 5), both indicated by an arrowhead in (a). For each of the mobility peaks detected, their associated m/z spectrum is also shown. Peaks were assigned following the considerations described in the Supplementary Text. ESI-IM-MS analysis of LMW_CL A β 40, LMW A β 42, and LMW_CL A β 42 samples is shown in Supplementary Figs S3–S5, respectively. Relative population of M (purple), D (orange), Tr (green), Te (blue), P (brown), and Hx (pink) in LMW A β 40 (empty bars), LMW A β 42 (filled bars), LMW_CL A β 40 (empty brick pattern bars) and LMW_CL A β 42 (filled bricked pattern bars) samples obtained from (d) the intensity counts of all charge states detected in ESI-IM-MS spectra.

of ESI-IM-MS for the characterization of A β oligomers, we next studied LMW and LMW_CL A β 40 and A β 42 samples in 10 mM ammonium acetate at pH 8.5 (Fig. 3 and Supplementary Figs S3–S5). We began ESI-IM-MS analysis by first assigning all the peaks in each spectrum to specific A β oligomers (see Supplementary Text). Briefly, assignments were performed on the basis of the ^{13}C isotope distribution (Fig. 3b,c and Supplementary Figs S3b,c–S5b,c), as proposed in the literature¹⁰. Whenever resolution was not enough, assignment was carried out by the detection of at least two consecutive charge states for a specific A β oligomer (Fig. 3a and Supplementary Figs S3a–S5a). The LMW and LMW_CL A β 40 and A β 42 samples ranged predominantly from monomers to trimers, although low intensity charge states for tetramers, pentamers and hexamers were also detected (M = monomers, D = dimers, Tr = trimers, Te = tetramers, P = pentamers, and Hx = hexamers) (Fig. 3a and Supplementary Figs S3a–S5a). Next, we determined the oligomer distribution in each sample by using all charge state ions across the whole spectrum (Fig. 3d). There were no significant differences between the oligomer distribution of A β 40 and A β 42 when compared in the LMW or LMW_CL samples. Hence, we concluded that the oligomer

distribution for A β 40 and A β 42 was the same, comprising mainly dimers and trimers, and that PICUP provided an accurate snapshot of this distribution. Noticeably, the ESI-IM-MS oligomer distribution was consistent with the GdnHSCN-SEC analysis (Supplementary Fig. S6), thereby supporting the reliability of ESI-IM-MS for the characterization of A β oligomers. Furthermore, in contrast to GdnHSCN-SEC analysis, ESI-IM-MS allowed detection of low abundant oligomers such as pentamers and hexamers and characterization of the oligomer order and distribution of non-covalently linked oligomers.

A β 40 and A β 42 dimers and trimers adopt a globular shape devoid of defined secondary structure. In addition to characterizing the A β oligomer order and distribution, ESI-IM-MS has the potential to identify chemical modifications, as well as to provide dynamic and structural information on the oligomers present in the sample. As per the characterization of chemical modifications, ESI-IM-MS analysis revealed that the mass of LMW_CL A β oligomers is consistent with the expected loss of two hydrogens for each covalent bond formed in the PICUP reaction (Supplementary Fig. S7)³⁵.

To establish the effect of cross-linking on A β oligomer dynamic, we measured the line width of the mobility peaks associated with specific A β oligomers. The line width corresponding to non-covalent A β oligomers in LMW samples was significantly larger than that of CL ones in LMW_CL samples (Supplementary Fig. S8). This finding indicated that during the mobility experiment each of the detected non-covalent A β oligomer sampled more conformations than their corresponding CL counterparts. A result consistent with the general expectation that cross-linking, which entails the formation of covalent bonds, reduces the number of accessible conformations.

Regarding structural information, ESI-IM-MS experiments can provide collisional cross-section (Ω) values^{8,11,22–24}, which are key structural constraints related to oligomer size and shape. We determined Ω for the most abundant A β oligomers detected in the LMW and LMW_CL A β 40 and A β 42 samples (Fig. 4a and Supplementary Table 2) and compared the same type of oligomer in the four samples. First, we compared the same type of oligomer in the LMW A β 40 and A β 42 samples and no significant differences in drift time (Supplementary Fig. S8a) or Ω values (Fig. 4a) were found, thereby indicating that they were similar. Next, we carried out, the same comparison for the LMW_CL A β 40 and A β 42 samples and found significant differences in drift time (Supplementary Fig. S8a) and Ω values (Fig. 4a). This result was not surprising since cross-linking reduces the conformational dynamics of A β oligomers (Supplementary Fig. S8) so we expected that differences in shape would be easier to distinguish among the CL oligomers than among the non-covalent ones. However, although this finding might indicate that LMW_CL A β 42 oligomers have a more extended structure than their A β 40 counterparts, the difference observed was consistent with the fact that A β 42 has two more amino acids than A β 40 (Supplementary Fig. S9). Accordingly, we concluded that A β 40 and A β 42 oligomers of the same order adopt the same shape, regardless of whether they are cross-linked.

To rationalize the experimentally obtained Ω values, we constructed three structural models of A β dimers for A β 40 (Fig. 4b) and A β 42 (Supplementary Fig. S10a). These models were built and named nuclear³⁶, fibrillar³⁷, or compact^{9,38}, on the basis of various structural restraints reported for A β aggregates. All the predicted Ω values (Fig. 4c and Supplementary Fig. S10b) were markedly larger than the experimental ones, thereby indicating that none of the proposed models fitted the experimental data. Thus, to build more realistic structural models and achieve better sampling, we ran atomistic molecular dynamics (MD) simulations using the replica exchange method (REMD) and simulation conditions similar to those in a ESI-MS experiment^{39,40}. In the first part of the simulations, all the models, irrespective of their original conformation, collapsed to adopt globular structures (Supplementary Fig. S11). Of the three structural models, the ensemble of globular structures for the nuclear form had the lowest energy (Supplementary Fig. S12). Thus, we took this low-energy ensemble to represent the structure of a globular dimer model (Fig. 4b and Supplementary Fig. S10a). The average Ω value of this ensemble was very similar to the experimental values obtained for the non-covalent and CL dimers (Fig. 4c and Supplementary Fig. S10b), thereby indicating that A β dimers have a globular shape. Next, to validate the lack of defined secondary structure adopted by the A β oligomers, we measured a CD spectrum of A β 40 and A β 42 CL dimers and trimers obtained immediately after SEC (Fig. 4d,e). The spectra for all four samples showed a minimum at around 200 nm, indicative of a lack of defined secondary structure. Additionally, an arm around 230 nm was also observed, which may reflect the existence of dynamic structural nuclei. In summary, the results from ESI-IM-MS, MD simulations, and CD spectroscopy were consistent with A β dimers and trimers adopting a globular shape devoid of defined secondary structure (Fig. 4 and Supplementary Fig. S10).

Discussion

Our results establish that SDS-PAGE leads to artifacts in the determination of the order and distribution of A β 42 oligomer samples and present ESI-IM-MS as a powerful technique to characterize the order, distribution, chemical modifications, and structure of both covalent and non-covalently linked A β oligomers (Fig. 5). Moreover, our findings indicate that pentamers and hexamers are artifacts of SDS-PAGE analysis and reveal A β 40 and A β 42 dimers and trimers, adopting a globular structure and lacking defined secondary structure, as the earliest oligomers formed during A β aggregation.

Although no other laboratory has studied LMW_CL A β 40 and A β 42 samples by ESI-IM-MS, they have addressed LMW A β 40 and A β 42 samples^{7,10}. In this regard, it is important to note that our results

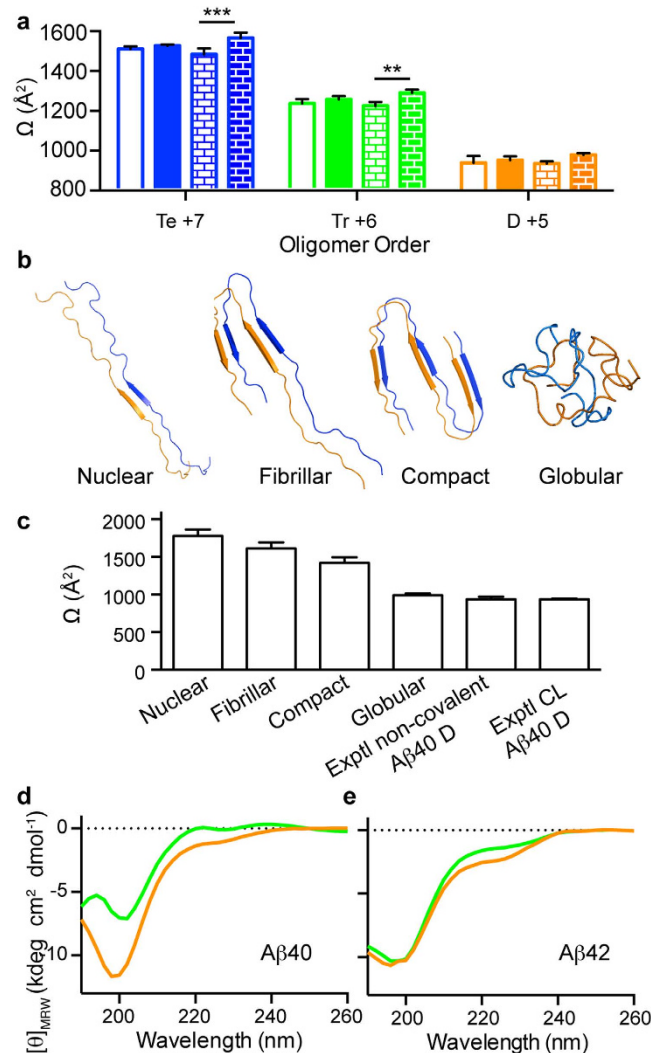


Figure 4. Aβ40 and Aβ42 dimers and trimers adopt a globular shape devoid of defined secondary structure. **(a)** Ω values obtained from the mobility peaks associated with the most abundant charge states for the most abundant Aβ oligomers detected (Te = tetramers, Tr = trimers, and D = dimers) Te +7 (blue), Tr +6 (green), and D +5 (orange) for LMW Aβ40 (empty bars), LMW Aβ42 (filled bars), LMW_CL Aβ40 (empty brick-pattern bars) and LMW_CL Aβ42 (filled brick-pattern bars). Data are the mean ± s.d. of three independent experiments. p-values are calculated using unpaired two-tailed Student's t-test (**p < 0.01 and ***p < 0.001). **(b)** Theoretical Aβ40 dimer models constructed using reported structural restraints for Aβ aggregates (nuclear³⁶, fibrillar³⁷, and compact^{9,38}), as well as those obtained from REMD simulations (globular). **(c)** Comparison of Ω values obtained from theoretical models of the dimer structures described in (b) with the experimental measures for the non-covalent and CL Aβ40 dimers reported in (a). **(d)** CD analysis of CL dimers (orange) and CL trimers (green) for **(d)** Aβ40 and **(e)** Aβ42 obtained after GdnHSCN-SEC fractionation.

are consistent only with studies that used the ¹³C isotopic distribution to assign peaks separated in the mobility dimension. This is the case for findings on LMW Aβ40 samples reported by Dadlez and co-workers¹⁰. They reported the presence of various oligomers, ranging from dimers to hexadecamers, adopting two conformations, namely compact and extended¹³. The Ω values for the oligomers detected in our study are in agreement with those reported by Dadlez's group. Differences in the number of oligomers detected in the two studies can be reconciled by taking into account that Dadlez's work was performed using a higher Aβ40 concentration (200 μM versus 30 μM). On the contrary, our results are not consistent with those of Bowers and co-workers⁷, who detected a single charge state (D -5, they work on negative mode) specific for an Aβ oligomer, which included various mobility peaks, assigned by the authors based upon injection energy studies and PICUP/SDS-PAGE experiments^{7,21}, to dimers and tetramers for Aβ40, and to dimers, tetramers, hexamers, and dodecamers for Aβ42. These same assignments were further repeated in subsequent papers from the group^{41–45}. Since their instrumentation

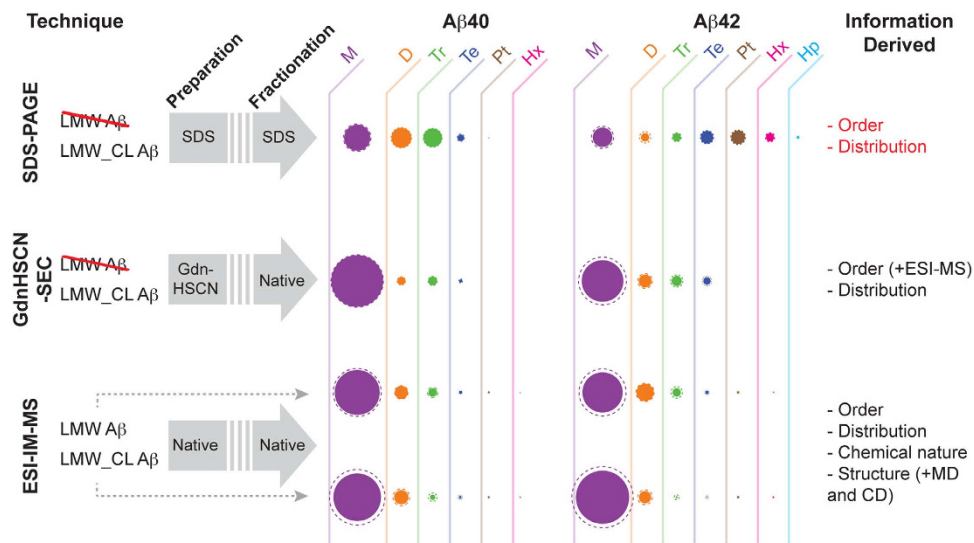


Figure 5. Schematics describing the conditions and the information derived from the different techniques used in this study to characterize LMW and LMW_CL A β samples. Techniques involving denaturing conditions in the preparation and/or fractionation of the samples are not suitable for the characterization of LMW A β samples. Filled and dashed circles indicate, respectively, the average and the standard deviation of the M = monomers (purple), D = dimers (orange), Tr = trimers (green), Te = tetramers (blue), P = pentamers (brown), Hx = hexamers (pink) and Hp = heptamers (cyan) relative population in each of the samples studied. The information obtained from each of the techniques is shown in the last column. Additional methods used to further support and/or validate specific information derived from either GdnHSCN-SEC or ESI-IM-MS are indicated in parentheses. The results derived from SDS-PAGE analysis are indicated in red because we have shown that this technique provides flawed information regarding the order and distribution of oligomers present in a sample (Fig. 2).

did not allow measuring the ^{13}C isotope distributions, they could not distinguish whether a mobility peak originated from a structural variant of an oligomer of the same order (*e.g.*, compact and extended forms) or from oligomers of distinct order. We indeed observed two mobility peaks associated with the D+5 charge state for A β 40 and A β 42 (Supplementary Fig. S13). However, on the basis of ^{13}C isotopic distribution, we assigned these peaks to compact and extended conformations of the dimer rather than to distinct oligomer forms. Therefore, an important conclusion for the application of ESI-IM-MS to the study of A β oligomers is that assignments should be based on the ^{13}C isotopic distribution of the peaks separated in the mobility dimension, as initially proposed by Dadlez and co-workers¹⁰. Whenever there is not enough resolution to determine the charge state, we propose that the detection of at least two consecutive charge states for a particular oligomer should be required to assign a mobility peak to a specific oligomer.

A key aspect of the present study is that the GdnHSCN-SEC strategy allowed us access to synthetic A β oligomers of well-defined order. This protocol greatly improves previous efforts to fractionate CL A β oligomers from SDS-PAGE bands. Indeed, a protocol for the isolation of CL A β oligomers of defined order from SDS-PAGE has been described for A β 40¹⁶. Attempts to apply the same protocol to CL A β 42 samples were unsuccessful¹⁶. According to the authors of that study, isolated CL A β 42 oligomers were not stable upon re-electrophoreses. This result reinforces our findings that A β 42 pentamers and hexamers are not *bona fide* cross-linked oligomers but are dimers and trimers that evolve into pentamers and hexamers in the presence of SDS. Having developed a fractionation protocol that permitted obtaining A β oligomers of well-defined order also allowed us to characterize them by CD spectroscopy. By combining CD analysis with structural information derived from Ω values obtained from ESI-IM-MS studies, and atomistic MD simulations, we show that dimers and trimers have a globular fold lacking defined secondary structure (Fig. 4 and Supplementary Fig. S10). This observation contrasts with previous publications where SDS-PAGE-purified CL A β 40 dimers, trimers, and tetramers were suggested to adopt a β -sheet structure¹⁶. In the aforementioned work, the authors used PICUP conditions that, in our hands, afforded a heterogeneous mixture of oxidized products when analyzed by RP-HPLC and LC-HRMS (Supplementary Fig. S1 and Table S1). Moreover, the authors fractionated the oligomers using SDS-PAGE, and although several purification steps were applied, there is the possibility that SDS contaminated the samples, thus affecting the structure of the purified oligomers.

In summary, our results reveal that SDS-PAGE leads to artifactual results in determining the order and distribution of A β 42 oligomers, while ESI-IM-MS is established as a powerful technique to characterize the order, distribution, chemical modifications, and structure of both covalent and non-covalently

linked A β 40 and A β 42 oligomers. These findings challenge previous scientific paradigms in the AD field built upon the use of SDS-PAGE to characterize A β oligomers samples. Among these paradigms, pentamers and hexamers have been established as the building blocks for A β aggregation. However, here we demonstrate that pentamers and hexamers form artifactually from dimers and trimers in the presence of SDS. Importantly, we identify A β 40 and A β 42 dimers and trimers, adopting a globular structure and lacking defined secondary structure, as the earliest oligomers formed during A β aggregation. This result is in agreement with an elegant study addressing homo- and hetero-molecular A β 40/A β 42 aggregation⁴⁶. This study reveals that from all possible stages of aggregation, A β 40 and A β 42 interact significantly only at the level of primary nucleation. The authors explain this result by suggesting that the structure of primary nuclei is less organized than that of the fibrils. This lower level of organization would allow for better accommodation of the two-residue C-terminal mismatch. Our findings indicating that A β 40 and A β 42 dimers and trimers adopt very similar shapes lacking defined secondary structure would be in complete agreement with the proposed explanation. Finally, since structural models for other higher order A β oligomers have been reported to adopt a β -sheet structure^{9,38,47}, our findings that A β dimers and trimers are globular and lack defined secondary structure indicate that major structural rearrangements occur during fibril formation. These observations highlight the importance of defining the structures and properties of the various species involved in A β aggregation. Indeed, it is only through this level of molecular detail that we will be able to interfere with A β aggregation in a rational manner.

Methods

Preparation of LMW A β 40 and A β 42. A β peptides of 40 and 42 residues, A β 40 and A β 42, were synthesized and purified by Dr. James I. Elliott (New Haven). LMW A β 40 and A β 42 preparations were obtained using Size-Exclusion Chromatography (SEC). A β peptide was dissolved in 6.8 M GdnHSCN (Life Technologies) at 8.5 mg/mL, sonicated for 5 min, and diluted to 5 mg/mL of peptide and 4 M GdnHSCN with H₂O. It was then centrifuged at 10,000 g for 6 min at 4 °C and passed through a 0.45- μ m Millex filter (Millipore). The resulting A β solution was injected into a HiLoad Superdex 75 prep grade column (GE Healthcare). The column was equilibrated using 10 mM sodium phosphate pH 7.4 and eluted at 4 °C at a flow rate of 1 mL/min. The peak attributed to LMW A β was collected and its protein concentration determined (see section Quantifying A β 40 and A β 42 protein concentration). The peptide solution was then diluted to 150 μ M, frozen, and kept at -20 °C until used.

Quantifying A β 40 and A β 42 protein concentration. LMW A β concentration obtained from SEC fractions was determined by reversed phase high-performance liquid chromatography (RP-HPLC) coupled to photodiode array detector (PDA) (Waters Alliance 2695 equipped with 2998 photodiode array detector). RP-HPLC analysis was carried out using a Symmetry 300 C₄ column (4.6 \times 150 mm, 5 μ m, 300 Å; Waters), a flow rate of 1 mL/min, and a linear gradient from 0 to 60% B in 15 min (A = 0.045% trifluoroacetic acid (TFA) in water, and B = 0.036% TFA in acetonitrile) at 60 °C. A calibration curve was generated based on A β 40 and A β 42 solutions that had previously been quantified by amino acid analysis.

Photo-Induced Cross-linking of Unmodified Proteins (PICUP). The PICUP reaction was initially run following descriptions in the literature³³. The experimental set-up consisted of a camera body and a 150-W slide projector. A PCR tube containing the reaction mixture to be cross-linked was placed inside the camera body for irradiation. The sample was irradiated via the slide projector for a short time, precisely controlled by the camera shutter. PICUP reactions were done using an A β /Ru(bpy)₃²⁺/APS ratio of 1:2:40. To this end, 4 μ L of 3 mM Ru(bpy)₃²⁺ and 4 μ L of 60 mM APS were added to 40 μ L of 150 μ M LMW A β in 10 mM sodium phosphate buffer. The mixture was irradiated for 1 s at a distance of 10 cm and immediately quenched by adding 6.5 μ L of 4 M dithiothreitol (DTT). Later on, reaction conditions were optimized to prevent A β oxidation (Supplementary Fig. S1). The best conditions were found when using a lower proportion of APS, A β /Ru(bpy)₃²⁺/APS 1:2:5, a distance of 10 cm, and an irradiation time of 1 s. Unless otherwise stated, we used an A β /Ru(bpy)₃²⁺/APS ratio of 1:2:5 to prevent formation of oxidized byproducts and to obtain chemically well-defined cross-linked oligomers. After the PICUP reaction, the reagents, which are incompatible with ESI-IM-MS and RP-HPLC analysis, were removed using Bio-Spin P30 columns (Bio-Rad) equilibrated in 10 mM ammonium acetate at pH 8.5. For comparative purposes, PICUP samples were also passed through Bio-Spin P30 columns when analyzed by SDS-PAGE.

SDS-PAGE. 10 μ L of 3X sample buffer (SB) (150 μ L 10% SDS, 75 μ L 4 M DTT, 400 μ L H₂O, 375 μ L 8X sample buffer -8 mL 1 M Tris pH 6.8, 9.3 mL 87% Glycerol, 5 mg Coomassie Brilliant Blue G, 2.8 mL H₂O) was added to 20 μ L of the sample to be analyzed by SDS-PAGE. The samples were boiled at 95 °C for 5 min, unless otherwise stated, and kept at -20 °C until used. A 20- μ L aliquot of each sample was electrophoresed in 0.75 mm-thick SDS-PAGE gels containing 15% acrylamide. Gels were run at 80–100 V and silver-stained.

RP-HPLC. RP-HPLC analysis of LMW_CL A β 40 samples was done using a Symmetry 300 C₄ column (4.6 × 150 mm, 5 μm, 300 Å; Waters) at a flow rate of 1 mL/min and a linear gradient from 0 to 60% B in 15 min (A = 0.045% TFA in water, and B = 0.036% TFA in acetonitrile) at 60 °C.

LC-HRMS. 180 pmols of LMW_CL A β 40 and LMW_CL A β 42 (Supplementary Fig. S14) were analyzed using a BioSuite pPhenyl 1000 analytical column (10 μm, 2 × 75 mm; Waters) at a flow rate of 100 μL/min comprising a linear gradient running from 5 to 80% B in 60 min (A = 0.1% formic acid (FA) in water, B = 0.1% FA in acetonitrile). The column outlet was directly connected to an Advion TriVersa NanoMate, which was used as a splitter and as the nanospray source of an LTQ-FT Ultra mass spectrometer (Thermo Scientific). Positive polarity was used with a spray voltage in the NanoMate source set to 1.7 kV. The capillary voltage, capillary temperature, and tube lens on the LTQ-FT were tuned to 40 V, 200 °C, and 100 V, respectively.

GdnHSCN-SEC. Although methionine oxidation was minimized by using A β /Ru(bpy)₃²⁺/APS ratios of 1:2:5, a small percentage of oxidized methionine was detected after isolation of CL A β dimers and trimers. To completely reduce all oxidized methionine side-chains, 500 μL of the quenched PICUP reaction were lyophilized and resuspended in TFA containing 30 equivalents of Me₂S-NH₄I and left for 2 hrs at 4 °C on a rotating wheel. Afterwards, TFA was evaporated under a stream of N₂ and 500 μL of H₂O was added to the sample. The mixture was then lyophilized, resuspended in 6.8 M GdnHSCN at an A β concentration of 8.5 mg/mL, and subsequently diluted with H₂O to 5 mg/mL of peptide and 4 M GdnHSCN. The resulting A β solution was injected into three columns in series, Superdex 75 HR 10/300-Superdex 75 HR 10/300-Superdex 200 HR10/300. The columns were equilibrated in 10 mM ammonium acetate pH 8.5, and the samples eluted at 4 °C at a flow rate of 0.5 mL/min.

ESI-IM-MS. ESI-IM-MS experiments were performed on a Synapt HDMS (Waters) quadrupole-traveling wave IMS-oaTOF mass spectrometer equipped with an Advion TriVersa NanoMate (Advion Biosciences). Positive ESI was used with a capillary voltage of 1.7 kV. A sampling cone voltage of 40 V and a backing pressure of 5.7 mbar were set for the observation of low-n A β oligomers. Although no signal was detected over 3000 m/z, data were acquired over the m/z range of 500 to 5000 for 2 min. The ion accelerating voltage in the trap T-wave device was 6 V unless otherwise stated; the ion accelerating voltage in the transfer T-wave device was kept constant at 4 V. The IM gas flow was kept at 23 mL/min. ESI-IM-MS data were obtained at three wave heights: 7, 7.5 and 8. The drift time Ω function was calibrated using denatured ubiquitin (charge states +9 to +11), myoglobin (charge states +15 to +22) and cytochrome C (charge states +11 to +18). Drift times were corrected for both mass-dependent and mass-independent times^{48,49}. All unknown drift time values, for which a Ω was derived, fell within the calibration curve obtained using the 19 charge states of the three protein standards. The raw data were processed using Mass Lynx v4.1 software (Waters). The reported data are the average of three independent experiments. The considerations to assign ESI-IM-MS peaks to specific A β oligomers are described in Supplementary text. To determine the low-n A β oligomer distribution for all four samples under study, we used all charge state ions across the whole spectra. For those charge states that contained contributions from different A β species in the mobility dimension, the relative contribution of each one was determined by fitting the mobilogram to a sum of Gaussian functions $g(x_c, w, A)$, where x_c , w , and A correspond to the center, the width at half-height, and the area of the Gaussian peak, respectively. The fitted function obtained for each mobilogram, f_{im} , can be written as:

$$f_{im} = k_{im} + \sum g(x_{cN}, w_N, A_N) \quad (1)$$

where k_{im} is the baseline intensity of the mobilogram, $\sum g(x_{cN}, w_N, A_N)$ is the sum of Gaussians contributing to each mobilogram, and N is the number of Gaussian/species used to fit each mobilogram. The relative population of a species contributing to a given charge state was obtained by dividing the area of the peak representing that species by the sum of the areas of each of the other species contributing to the given charge state. The contribution of a species to the overall intensity of a charge state ion was obtained by multiplying it by its relative population. The population of a species was obtained by summing the intensity of all charge states specific for the particular species and dividing it by the sum of the intensities of all charge state ions across the whole spectra.

Modeling A β dimer structure. *Construction of A β dimer models.* Three structural models for A β 40 and A β 42 dimers were built, taking into account reported structural restraints for A β aggregates (nuclear³⁶, fibrillar³⁷, and compact^{9,38}) (Fig. 4b for A β 40, Supplementary Fig. S10a for A β 42). The sequence of A β was divided into three segments: the N-terminus (residues 1 to 11), the middle segment (residues 12 to 26), and the C-terminus (residues 27 to 40 for A β 40, or 27 to 42 for A β 42). In all the models, the two A β units interact through β -strand regions defined within each A β unit to form parallel β -sheets through intermolecular hydrogen bonds. Previous reports have proposed that the region comprising residues 17 to 21 nucleates A β self-assembly³⁶. In the nuclear model, residues 12 to 24 adopt a β -strand conformation. In the fibrillar model, the regions spanning residues 12 to 24 and residues 30 to 40 (for A β 40) or 42 (for A β 42) adopt a β -strand conformation. Residues 25–29 contain a bend that

brings the two β -strands into contact through side chain-side chain interactions. This model corresponds to the structure of A β when it is incorporated into the fibril³⁷. The compact model was constructed taking into account structural models of specific A β oligomer preparations that reveal a stable N-terminal β -strand^{9,38}. Thus, each A β unit contained three β -strand regions comprising residues 1 to 6, 12 to 24, and 30 to 40 (for A β 40) or 42 (for A β 42). Residues 7 to 11 and 25 to 29 include a bend of the peptide that brings the three β -strands into contact through side chain-side chain interactions. Each of the six structural models, three for A β 40 and three for A β 42, were constructed using PyMol and Modeller tools starting from the A β 40 fibril structure derived from solid-state Nuclear Magnetic Resonance Spectroscopy (ssNMR) data (Protein Data Bank ID is 2LMN)³⁷.

Structure equilibration in water. The six structural models were built, optimized, solvated in a truncated octahedron box, and then subsequently neutralized with six sodium ions⁵⁰. Transferable Interaction Potential 3 point (TIP3P)⁵¹ parameters were used for water and AMBER99SB-ILDN force field⁵² for proteins. Simulations in water were done using periodic boundary conditions and the particle mesh Ewald method⁵³ for long-range electrostatic treatment (0.12 nm grid size), combined with a cut-off radius of 1 nm for Lennard-Jones interactions. All aqueous simulations were done at the isothermal-isobaric ensemble (T = 300 K and P = 1 atm) using a Berendsen thermostat and barostat⁵⁴. The SHAKE algorithm⁵⁵ was used to constrain all bond distances to their equilibrium value, allowing a 2-fs integration time step for solution conditions. We performed 5 ns of equilibration in water and computed and minimized the averaged structure of snapshots collected in the last ns. Ω values for each of the structural models were computed with the exact hard sphere scattering method (EHSS), which consists of a trajectory calculation using hard spheres centered at the position of each atom⁵⁶.

REMD simulation in the gas phase. As a starting structure for REMD simulation, water molecules and counter ions were removed. We used the REMD method⁵⁷ to perform extended simulations at a range of temperatures for the three models of A β 40 and A β 42 dimers in the gas phase. The simulations were done considering a charge state +5, which is the most populated charge state for dimers in the ESI-MS profile. We chose 19 simulation temperatures for each structure, covering a range from 300 K to 614 K, which corresponds to the temperature variability range in the mobility measurements⁵⁸. For gas phase simulations, we did not use any cut-off for non-bonded interactions. We used the SHAKE algorithm for constraining bonds and a 1-fs integration time step. For each A β dimer structure, we performed 1 μ s of REMD simulation. For the analysis, we considered the trajectories at 300 K, a temperature that simulates ideally mild vaporization conditions, and used the Gromacs.4.5.3 package. Ω values for the ensemble of structures generated during the last 500 ns of REMD, were also computed with the exact hard sphere scattering method (EHSS)⁵⁶.

Far-UV CD Spectroscopy. CD spectra were recorded on a Jasco 815 spectrometer from 190 to 250 nm with a data pitch of 0.2 nm, a bandwidth of 2 nm, and a scan speed of 50 nm/min with a 4-s response time. A 1-cm cell was used. After GdnHSCN-SEC fractionation using three columns in series equilibrated in 10 mM sodium phosphate at pH 8.5, spectra for CL A β 40 and A β 42 dimers, and trimers were acquired at 4 °C. CD data were analyzed using the SpectraManager program.

Summary of statistical analysis. GraphPad Prism was used for all statistical analyses. The data are presented as mean \pm s.d. except when stated otherwise. The Student's t-test (unpaired, two-tailed) was used to calculate statistical significance. The images shown are representative of those obtained in at least three independent experiments.

References

- Haass, C. & Selkoe, D. J. Soluble protein oligomers in neurodegeneration: lessons from the Alzheimer's amyloid beta-peptide. *Nat. Rev. Mol. Cell Biol.* **8**, 101–112 (2007).
- Hefli, F. *et al.* The case for soluble Abeta oligomers as a drug target in Alzheimer's disease. *Trends Pharmacol. Sci.* **34**, 261–266 (2013).
- Editorial. State of aggregation. *Nat. Neurosci.* **14**, 399 (2011).
- Benilova, I., Karran, E. & De Strooper, B. The toxic Abeta oligomer and Alzheimer's disease: an emperor in need of clothes. *Nat. Neurosci.* **15**, 349–357 (2012).
- Bitan, G. *et al.* Amyloid beta-protein (Abeta) assembly: Abeta 40 and Abeta 42 oligomerize through distinct pathways. *Proc. Natl. Acad. Sci. USA* **100**, 330–335 (2003).
- Necula, M., Kaye, R., Milton, S. & Glabe, C. G. Small molecule inhibitors of aggregation indicate that amyloid beta oligomerization and fibrillization pathways are independent and distinct. *J. Biol. Chem.* **282**, 10311–10324 (2007).
- Bernstein, S. L. *et al.* Amyloid-beta protein oligomerization and the importance of tetramers and dodecamers in the aetiology of Alzheimer's disease. *Nat. Chem.* **1**, 326–331 (2009).
- Yu, L. *et al.* Structural characterization of a soluble amyloid beta-peptide oligomer. *Biochemistry* **48**, 1870–1877 (2009).
- Ahmed, M. *et al.* Structural conversion of neurotoxic amyloid-beta(1-42) oligomers to fibrils. *Nat. Struct. Mol. Biol.* **17**, 561–567 (2010).
- Kloniecki, M. *et al.* Ion mobility separation coupled with MS detects two structural states of Alzheimer's disease Abeta1-40 peptide oligomers. *J. Mol. Biol.* **407**, 110–124 (2011).
- Lee, J., Culyba, E. K., Powers, E. T. & Kelly, J. W. Amyloid-beta forms fibrils by nucleated conformational conversion of oligomers. *Nat. Chem. Biol.* **7**, 602–609 (2011).

12. Narayan, P. *et al.* The extracellular chaperone clusterin sequesters oligomeric forms of the amyloid-beta(1–40) peptide. *Nat. Struct. Mol. Biol.* **19**, 79–83 (2012).
13. Bitan, G. & Teplow, D. B. Rapid photochemical cross-linking—a new tool for studies of metastable, amyloidogenic protein assemblies. *Acc. Chem. Res.* **37**, 357–364 (2004).
14. Citron, M. *et al.* Mutant presenilins of Alzheimer's disease increase production of 42-residue amyloid beta-protein in both transfected cells and transgenic mice. *Nat. Med.* **3**, 67–72 (1997).
15. Blennow, K., Zetterberg, H. & Fagan, A. M. Fluid biomarkers in Alzheimer disease. *Cold Spring Harb. Perspect. Med.* **2**, a006221 (2012).
16. Ono, K., Condron, M. M. & Teplow, D. B. Structure-neurotoxicity relationships of amyloid beta-protein oligomers. *Proc. Natl. Acad. Sci. USA* **106**, 14745–14750 (2009).
17. Paravastu, A. K., Qahwash, I., Leapman, R. D., Meredith, S. C. & Tycko, R. Seeded growth of beta-amyloid fibrils from Alzheimer's brain-derived fibrils produces a distinct fibril structure. *Proc. Natl. Acad. Sci. USA* **106**, 7443–7448 (2009).
18. Roychoudhuri, R., Yang, M., Hoshi, M. M. & Teplow, D. B. Amyloid beta-protein assembly and Alzheimer disease. *J. Biol. Chem.* **284**, 4749–4753 (2009).
19. Bitan, G., Fradinger, E. A., Spring, S. M. & Teplow, D. B. Neurotoxic protein oligomers—what you see is not always what you get. *Amyloid* **12**, 88–95 (2005).
20. Watt, A. D. *et al.* Oligomers, fact or artefact? SDS-PAGE induces dimerization of beta-amyloid in human brain samples. *Acta Neuropathol.* **125**, 549–564 (2013).
21. Bernstein, S. L. *et al.* Amyloid beta-protein: monomer structure and early aggregation states of Abeta42 and its Pro19 alloform. *J. Am. Chem. Soc.* **127**, 2075–2084 (2005).
22. Smith, D. P., Radford, S. E. & Ashcroft, A. E. Elongated oligomers in beta2-microglobulin amyloid assembly revealed by ion mobility spectrometry-mass spectrometry. *Proc. Natl. Acad. Sci. USA* **107**, 6794–6798 (2010).
23. Sitkiewicz, E., Oledzki, J., Poznanski, J. & Dadlez, M. Di-tyrosine cross-link decreases the collisional cross-section of Abeta peptide dimers and trimers in the gas phase: an ion mobility study. *PLoS one* **9**, e100200 (2014).
24. Sitkiewicz, E., Klonecki, M., Poznanski, J., Bal, W. & Dadlez, M. Factors influencing compact-extended structure equilibrium in oligomers of Abeta1–40 peptide—an ion mobility mass spectrometry study. *J. Mol. Biol.* **426**, 2871–2885 (2014).
25. Hernandez, H. & Robinson, C. V. Determining the stoichiometry and interactions of macromolecular assemblies from mass spectrometry. *Nat. Protoc.* **2**, 715–726 (2007).
26. Ayed, A., Krutchinsky, A. N., Ens, W., Standing, K. G. & Duckworth, H. W. Quantitative evaluation of protein-protein and ligand-protein equilibria of a large allosteric enzyme by electrospray ionization time-of-flight mass spectrometry. *Rapid Commun. Mass Spectrom.* **12**, 339–344 (1998).
27. Gabelica, V., Galic, N., Rosu, F., Houssier, C. & De Pauw, E. Influence of response factors on determining equilibrium association constants of non-covalent complexes by electrospray ionization mass spectrometry. *J. Mass Spectrom.* **38**, 491–501 (2003).
28. Chitta, R. K., Rempel, D. L. & Gross, M. L. Determination of affinity constants and response factors of the noncovalent dimer of gramicidin by electrospray ionization mass spectrometry and mathematical modeling. *J. Am. Soc. Mass Spectrom.* **16**, 1031–1038 (2005).
29. Liu, J. & Konermann, L. Protein-protein binding affinities in solution determined by electrospray mass spectrometry. *J. Am. Soc. Mass Spectrom.* **22**, 408–417 (2011).
30. Boeri Erba, E., Barylyuk, K., Yang, Y. & Zenobi, R. Quantifying protein-protein interactions within noncovalent complexes using electrospray ionization mass spectrometry. *Anal. Chem.* **83**, 9251–9259 (2011).
31. Teplow, D. B. Preparation of amyloid beta-protein for structural and functional studies. *Methods Enzymol.* **413**, 20–33 (2006).
32. Jan, A., Hartley, D. M. & Lashuel, H. A. Preparation and characterization of toxic Abeta aggregates for structural and functional studies in Alzheimer's disease research. *Nat. Protoc.* **5**, 1186–1209 (2010).
33. Bitan, G. Structural study of metastable amyloidogenic protein oligomers by photo-induced cross-linking of unmodified proteins. *Methods Enzymol.* **413**, 217–236 (2006).
34. Selkoe, D. J., Abraham, C. R., Podlisky, M. B. & Duffy, L. K. Isolation of low-molecular-weight proteins from amyloid plaque fibers in Alzheimer's disease. *J. Neurochem.* **46**, 1820–1834 (1986).
35. Fancy, D. A. & Kodadek, T. Chemistry for the analysis of protein-protein interactions: rapid and efficient cross-linking triggered by long wavelength light. *Proc. Natl. Acad. Sci. USA* **96**, 6020–6024 (1999).
36. Reinke, A. A., Ung, P. M., Quintero, J. J., Carlson, H. A. & Gestwicki, J. E. Chemical probes that selectively recognize the earliest Abeta oligomers in complex mixtures. *J. Am. Chem. Soc.* **132**, 17655–17657 (2010).
37. Petkova, A. T., Yau, W. M. & Tycko, R. Experimental constraints on quaternary structure in Alzheimer's beta-amyloid fibrils. *Biochemistry* **45**, 498–512 (2006).
38. Haupt, C. *et al.* Structural basis of beta-amyloid-dependent synaptic dysfunctions. *Angew. Chem. Int. Ed. Engl.* **51**, 1576–1579 (2012).
39. Arcella, A. *et al.* Structure and dynamics of oligonucleotides in the gas phase. *Angew. Chem. Int. Ed. Engl.* **54**, 467–471 (2015).
40. Meyer, T., Gabelica, V., Grubmüller, H. & Orozco, M. Proteins in the gas phase. *WIREs Comput. Mol. Sci.* **3**, 408–425 (2012).
41. Murray, M. M. *et al.* Amyloid beta protein: Abeta40 inhibits Abeta42 oligomerization. *J. Am. Chem. Soc.* **131**, 6316–6317 (2009).
42. Gessel, M. M., Bernstein, S., Kemper, M., Teplow, D. B. & Bowers, M. T. Familial Alzheimer's disease mutations differentially alter amyloid beta-protein oligomerization. *ACS Chem. Neurosci.* **3**, 909–918 (2012).
43. Gessel, M. M. *et al.* Abeta(39–42) modulates Abeta oligomerization but not fibril formation. *Biochemistry* **51**, 108–117 (2012).
44. Zheng, X. *et al.* Z-Phe-Ala-diazomethylketone (PADK) disrupts and remodels early oligomer states of the Alzheimer disease Abeta42 protein. *J. Biol. Chem.* **287**, 6084–6088 (2012).
45. Zheng, X. *et al.* Amyloid beta-protein assembly: The effect of molecular tweezers CLR01 and CLR03. *J. Phys. Chem. B* **119**, 4831–4841 (2015).
46. Cukalevski, R. *et al.* The A β 40 and A β 42 peptides self-assemble into separate homomolecular fibrils in binary mixtures but cross-react during primary nucleation. *Chem. Sci.* **6**, 4215–4233 (2015).
47. Lendel, C. *et al.* A hexameric peptide barrel as building block of amyloid-beta protofibrils. *Angew. Chem. Int. Ed. Engl.* **53**, 12756–12760 (2014).
48. Ruotolo, B. T., Benesch, J. L., Sandercock, A. M., Hyung, S. J. & Robinson, C. V. Ion mobility-mass spectrometry analysis of large protein complexes. *Nat. Protoc.* **3**, 1139–1152 (2008).
49. Smith, D. P. *et al.* Deciphering drift time measurements from travelling wave ion mobility spectrometry-mass spectrometry studies. *Eur. J. Mass Spectrom.* **15**, 113–130 (2009).
50. Smith, D. E. & Dang, L. X. Computer simulations of NaCl association in polarizable water. *J. Chem. Phys.* **100**, 3757–3766 (1994).
51. Jorgensen, W. L., Chandrasekhar, J., Madura, J. D., Impey, R. W. & Klein, M. L. Comparison of Simple Potential Functions for Simulating Liquid Water. *J. Chem. Phys.* **79**, 926–935 (1983).
52. Lindorff-Larsen, K. *et al.* Improved side-chain torsion potentials for the Amber ff99SB protein force field. *Proteins* **78**, 1950–1958 (2010).

53. York, D. M., Darden, T. A. & Pedersen, L. G. The effect of long-range electrostatic interactions in simulations of macromolecular crystals: A comparison of the Ewald and truncated list methods. *J. Chem. Phys.* **99**, 8345–8348 (1993).
54. Berendsen, H. J. C., Postma, J. P. M., van Gunsteren, W. F., DiNola, A. & Haak, J. R. Molecular dynamics with coupling to an external bath. *J. Chem. Phys.* **81**, 3684–3690 (1984).
55. Ryckaert, P., Cicotti, G. & Berendsen, H. J. C. Numerical Integration of the Cartesian Equations of Motion of a System with Constraints: Molecular Dynamics of n-Alkanes. *J. Comput. Phys.* **23**, 327–341 (1977).
56. Shvartsburg, A. A. & Jarrold, M. F. An exact hard-spheres scattering model for the mobilities of polyatomic ions. *Chem. Phys. Lett.* **261**, 86–91 (1996).
57. Sugita, Y. & Okamoto, Y. Replica-exchange molecular dynamics method for protein folding. *Chem. Phys. Lett.* **314**, 141–151 (1999).
58. Morsa, D., Gabelica, V. & De Pauw, E. Effective temperature of ions in traveling wave ion mobility spectrometry. *Anal. Chem.* **83**, 5775–5782 (2011).

Acknowledgments

R.P. and S.V. acknowledge IRB Barcelona and the Spanish Government FPI programs, respectively, for predoctoral fellowships. We thank Prof. Ernest Giralt for helpful discussions and critical reading of the manuscript, Dr. Sergio Madurga for generating preliminary models for comparison against experimental Ω and helping with Gaussian fitting, Dr. Marina Gay and Mar Vilanova for mass spectrometry support, and T. Yates for editorial help. N.C. and M.V. are active participants and MC members of the European COST Action BM 1403. IRB Barcelona Mass Spectrometry Core Facility is a ProteoRed laboratory, part of PRB2-ISCI, supported by grant PT13/0001. This work was supported by grants from MINECO-FEDER (SAF2012-35226) and from the Alzheimer's Association (NIRP-12-256641), both to N.C.

Author Contributions

R.P. and S.V. optimized PICUP conditions for preparing chemically well-defined LMW-CL A β samples. S.V. designed, performed, and analyzed the results of SDS-PAGE analysis. S.V. and R.M. designed and implemented the GdnHSCN-SEC protocol. R.P. designed, performed, and analyzed ESI-IM-MS experiments. S.V. obtained oligomer distribution from ESI-IM-MS data. Regarding the construction of A β dimer models and atomistic MD simulations, A.A. and M.O. designed the experiments, A.A. performed them, and A.A. and M.O. analyzed the data. M.V. performed LC-HRMS and ESI-MS experiments and gave technical support and conceptual advice on the ESI-IM-MS experiments. S.V. and R.M. designed, performed, and analyzed the results of CD experiments. N.C. conceived the study, designed and oversaw all experiments, and wrote the manuscript. All the authors discussed the results, and commented on and contributed to sections of the manuscript.

Additional Information

Supplementary information accompanies this paper at <http://www.nature.com/srep>

Competing financial interests: The authors declare no competing financial interests.

How to cite this article: Pujol-Pina, R. *et al.* SDS-PAGE analysis of A β oligomers is disserving research into Alzheimer's disease: appealing for ESI-IM-MS. *Sci. Rep.* **5**, 14809; doi: 10.1038/srep14809 (2015).



This work is licensed under a Creative Commons Attribution 4.0 International License. The images or other third party material in this article are included in the article's Creative Commons license, unless indicated otherwise in the credit line; if the material is not included under the Creative Commons license, users will need to obtain permission from the license holder to reproduce the material. To view a copy of this license, visit <http://creativecommons.org/licenses/by/4.0/>